The Continuum in 5-Fluorocytosine. Toward Salt Formation

ARTICLE *in* CRYSTAL GROWTH & DESIGN · SEPTEMBER 2013

Impact Factor: 4.89 · DOI: 10.1021/cg400662n

CRYSTAL GROWTH & DESIGN

Article

pubs.acs.org/crystal

The Continuum in 5-Fluorocytosine. Toward Salt Formation

Cecília C. P. da Silva,[†] Rebeka de Oliveira,[†] Juan C. Tenorio,[†] Sara B. Honorato,[‡] Alejandro P. Ayala,[‡] and Javier Ellena*[,†]

[†]Instituto de Física de São Carlos, Universidade de São Paulo, CP 369, 13560-970, São Carlos, São Paulo, Brazil

[‡]Departamento de Física, Universidade Federal do Ceará, CP 6030, 60455-970 Fortaleza, Ceará, Brazil

Supporting Information

ABSTRACT: 5-Fluorocytosine (5-FC) was crystallized with complementary dicarboxylic acids, aiming to achieve a controlled synthesis of structures based on the ΔpK_a rule proposed in the salt−cocrystal continuum study and to provide structural information helpful in the comprehension of its supramolecularity. Although 5-FC tends to be basic, pK_a = 3.26, only three salts are reported. In this way, new 5-FC salts were obtained, the fumaric, maleic and oxalic ones, all crystallizing in the monoclinic space group $P2_1/c$. In the 5-FC oxalate and fumarate cases, the acid molecules are placed on an inversion center in a fashion that each half molecule exhibits one terminal donor−acceptor site, leading to the constitution of a 5-FC−acid−5-FC heterodimer. Such a heterodimer is observed in only one donor−acceptor site of the maleate of 5-FC, whose acid molecule exhibits a closed chain architecture. Infrared and Raman spectra recorded for the three compounds complement the salt characterization on the basis of the extent of proton transfer. Thermal analysis evidence that the salt formation decreases the melting point of the new compounds, ranking this molecule as a coformer candidate to improve the physical properties of other drugs.

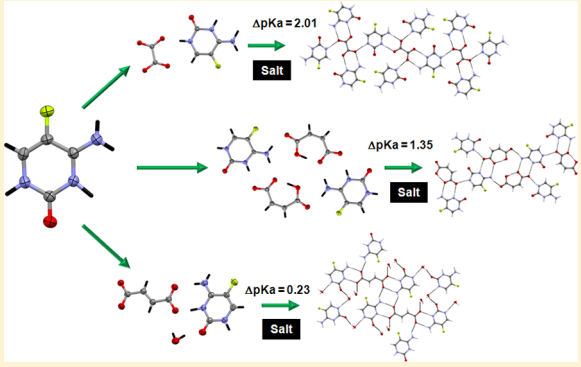

1. INTRODUCTION

Pharmaceutical salts are composed of at least one molecular cationic or anionic active pharmaceutical ingredient (API) and one molecular or monatomic counterion, having the charge balance to possess a definite stoichiometry.[1] They have been preferred for the pharmaceutical industry for a long period because they offer preferential properties in comparison with their parent molecules such as increased chemical stability, solubility, and dissolution rates.[2] In the past few years, the term pharmaceutical cocrystal has emerged in scientific publications worldwide, referring to crystalline structures composed by neutral molecular components, usually involving an API and one cocrystal former, also exhibiting a definite stoichiometry ratio, often leading to a hydrogen-bonded molecular complex. The main distinction between salts and cocrystals is based on the charge transfer ratio occurring among the API and the guest molecule: if the proton involved in the hydrogen-bonding interaction is transferred from the donor to the acceptor, a salt is formed and, on the contrary, a cocrystal is generated.[1,3]

However, when acid−base complexes exhibit similar values of pK_a, a problem emerges, and the decision if the new compound is a salt or a cocrystal is not possible. In an attempt to predict the influence of the crystal contents on the ionization states of the molecules, i.e., to evaluate the extend of proton transfer in the solid state aiming to establish if a salt or a cocrystal will be formed, Childs et al.[4] performed a study involving a total of 20 complexes with theophylline, proposing modifications in the ΔpK_a rules. The proposed guideline is known by "rule of three" and states that salts are expected if the ΔpK_a ($pK_{a-(base)} - pK_{a(acid)}$) is greater than 2 or 3 units. Nangia et al.[5] noted that if the ΔpK_a was smaller than 0, cocrystal formation was expected. Therefore, ΔpK_a ranging between 0 and 2 or 3 are considered to be in a salt−cocrystal continuum, having the extension of proton transfer between the compounds decided on the basis of C−O bond distances. Recently, an extensive work based on salt−cocrystal design considered that there is poor predictive power on the salt−cocrystal continuum and that it is different among systems.[6] On the other hand, Perumalla et al.[7] were able to control the synthesis of two protonated states of cytosine and 5-fluorocytosine structures by manipulating the pK_a and the concentration of the acids used for the salt formation.

5-Fluorocytosine (4-amino-5-fluoro-1,2-dihydropyrimidin-2-one, 5-FC, Scheme 1) is an antimetabolite widely used as an antifungal agent, acting by the deamination of 5-FC into 5-fluorouracil (5-FU) by the enzyme cytosine deaminase (CD) present in the fungal cells.[8] 5-FU is a potent, but highly toxic, antineoplastic agent used for topical treatment of superficial basal cell carcinomas and injected to treat some types of cancer such as gastric, breast, head, neck, rectal, etc.[9,10] In 1985, 5-FC

Received: April 30, 2013
Revised: August 20, 2013
Published: September 3, 2013

dx.doi.org/10.1021/cg400662n | *Cryst. Growth Des.* 2013, 13, 4315−4322

Scheme 1. Molecular Structure of 5-FC

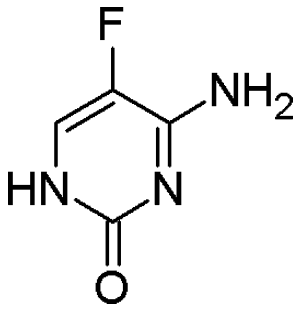

was introduced in combination with CD for cancer treatment.[8,11] The activation of 5-FC in tumor tissues is accomplished by gene-directed enzyme prodrug therapy (GDEPT). In this technique, the CD gene is delivered into the tumor cells and expressed on it, enabling systematically administered 5-FC to be converted into 5-FU inside these cells, killing the tumor.[12]

Although 5-FC tends to be basic (pK_a = 3.26), only three protonated structures were reported, a salicylate and two chloride monohydrates,[7,13,14] against two polymorphs,[15] seven hydrates,[15−19] four solvates,[15,17] and thirteen cocrystals (including eight solvated cocrystals).[20−22] In an effort to contribute with the salt−cocrystal continuum study and attempting to provide information helpful toward the comprehension of the chemical features that lead 5-FC to form salts or cocrystals, particularly in the continuum, we worked with dicarboxylic acids exhibiting pK_a values in such a way that the ΔpK_a ranged from close to 0 until close to 2: oxalic (pK_a = 1.25), maleic (pK_a = 1.91), and fumaric (pK_a = 3.03) acids.

2. EXPERIMENTAL SECTION

5-FC was purchased from Sigma-Aldrich Brazil and used without further purification. Reagents were purchased from commercial vendors and also used without purification. Milli-Q water, acetonitrile, and 2-propanol were used as solvents. The resulting salts were analyzed by single crystal X-ray diffraction, X-ray powder diffraction, hot-stage microscopy, thermal analysis, and spectroscopic studies.

2.1. Synthesis of the Crystals. 5-FC was dissolved, under stirring using a magnet, with oxalic, fumaric, and maleic acids in an equimolar ratio (0.07 mmol) in 1 mL of hot water (60 °C) until the complete dissolution of the solids. Next, the hot mixtures were filtered through a 0.45 μm filter (Milipore), and the resulting solutions were maintained at room temperature, semicovered by Parafilm until complete slow evaporation of the solvent. After 24 h, colorless, plate-shaped crystals of 5-FC with oxalic acid started to grow inside the solution. The complete evaporation of the solvent occurred after 14 days, and crystals were collected for the experiments. For the 5-FC experiments with the fumaric and the maleic acids, the crystals grew only after 12 and 15 days, respectively, i.e., after the complete evaporation of the solvent. The crystallization experiments were repeated at 4 °C. Others crystallization conditions were also used, like solutions of water/acetonitrile (1:1) and water/2-propanol (1:1). These experiments were performed at room temperature as well as at 4 °C.

The above proceedings were adopted as an attempt to analyze the dependence of salt−cocrystal formation under different experimental conditions. It is worth mentioning that lower temperatures were not considered for the experiments to avoid problems with the water freezing.

2.2. Powder X-ray Diffraction (PXRD). bulk samples were analyzed using a Rigaku−Denki powder diffractometer. Experimental conditions: Cu Kα radiation, λ = 1.5418 Å; 50 kV; 100 mA; step scan with a step width of 0.01° in an interval of 10−50° in 2θ; time per step 3 s. Experimental and calculated PXRD patterns were compared in order to confirm if the composition of each bulk material was consistent with that used in the single crystal X-ray diffraction analysis.

2.3. Single Crystal X-ray Structure Determination. X-ray diffraction data collection (φ scans and ω scans with κ offsets) were performed on an Enraf−Nonius Kappa−CCD diffractometer (95 mm CCD camera on κ-goniostat) using graphite-monochromated Mo Kα radiation (0.71073 Å). Intensity data were collected at 100.0(2)K, using the Oxford Cryosystem cryogenic device. The software COLLECT[23] and Denzo−Scalepack package of softwares[24] were applied for acquisition, indexing, integration, and scaling of Bragg reflections. The final cell parameters were obtained using all reflections. No absorption correction was applied. The structures were solved by direct methods, and the models obtained were refined by full-matrix least-squares on F^2 (SHELXL-97[25]) using the WinGX v1.70.01[26] program packages. Hydrogen atoms were stereochemically positioned and refined with fixed individual displacement parameters [U_{iso}(H) = 1.2U_{eq}] according to the riding model (C−H bond lengths of 0.93 Å), except for the N^+−H and O−H ones, which were located on the difference Fourier maps and refinement of their positions with fixed isotropic thermal parameters was performed (U_{iso}(H) = 1.2U_{eq}(N) or 1.5U_{eq}(O)).

The programs MERCURY (version 2.3)[27] and ORTEP-3[28] were used within WinGX v1.70.01[26] to prepare the crystallographic information files (CIF) and artwork representations for publication. The CIFs of the three 5-FC structures were deposited with the Cambridge Structural Data Base under the codes CCDC 915469, 915470, and 915471, for oxalate of 5-FC, maleate of 5-FC and fumarate monohydrate of 5-FC, respectively. Copies of these files may be solicited free of charge from The Director, CCDC, 12 Union Road, Cambridge CB2 1EZ, UK; fax, + 441223-336033; e-mail, deposit@ccdc.cam.ac.uk or http:www.ccdc.cam.ac.uk.

2.4. Hot-Stage Polarized Optical Microscopy. Microscopy was performed on a Leica DM2500P microscope connected to the Linkam T95-PE hot-stage equipment. Data were visualized with the Linksys 32 software for hot stage control. One crystal of each sample was placed on a 13 mm glass coverslip, placed on a 22 mm diameter pure silver heating block inside of the stage. The sample was heated at a ramp rate of 10 °C/min up to a final temperature of 300 °C but discontinued on melting of all material.

2.5. Thermal Analysis. Differential scanning calorimetry (DSC) curves were obtained using a Shimadzu TA-60WS thermal analysis system, where the samples were loaded in aluminum pans (2−5 mg) and heated from room temperature up to 296 °C, at 10 °C·min^{-1}, under nitrogen flow (50 mL min^{-1}). Thermogravimetric (TG) curve for the fumarate monohydrate of 5-FC was obtained using a Shimadzu TGA-50, where 4.6 mg of sample was loaded in an alumina pan and heated from room temperature up to 180 °C, at 10 °C·min^{-1}, under nitrogen flow (50 mL min^{-1}).

2.6. Vibrational Spectroscopy. Fourier transform infrared (FT-IR) spectra were recorded at a spectral resolution of 4 cm^{-1} using a Bruker VERTEX 70 spectrometer. Samples of oxalate of 5-FC, fumarate monohydrate of 5-FC, and maleate of 5-FC were analyzed by the transmission technique as KBr pellets prepared using a hydraulic press (mixtures comprising 200 mg of KBr and 1 mg of each sample). Raman spectra were recorded in a Jobin Yvon LabRam HR spectrometer equipped with a liquid nitrogen refrigerated CCD detector. A HeNe laser was used as excitation source.

2.7. Quantum Mechanical Calculations. Quantum chemistry theoretical calculations of the potential energy surface (PES) scan were performed to explore the influence of the proton displacement between the 5-FC (nucleic base) and the carboxylic acids on the energy of the ionic pair. The electronic structure and optimized geometry were computed within the density functional theory employing a hybrid of Becke's nonlocal three-parameter exchange functional and the Lee−Yang−Parr correlation functional (B3LYP)[29−31] and Hartree−Fock HF level of theory[32] using Gaussian 03.[33] The spent energy of proton displacement was evaluated by using the 6-311++G and the 6-31++G basis set, calculated by 20 steps varying in intervals of 0.1 Å.

3. RESULTS

3.1. Structural Description. To simplify the discussion concerning the new 5-FC crystalline structures, the following nomenclature will be applied: form O (oxalate of 5-FC), form Ma (maleate of 5-FC), and form F (fumarate monohydrate of 5-FC). The crystallographic data for the structures are summarized in the Table 1.

Table 1. Crystallographic Data for the 5-FC Forms O, Ma, and F

form O $C_4H_5FN_3O^+$, $^1/_2C_2O_4^-$	form Ma $2C_4H_5FN_3O^+$, $2C_4H_3O_4^-$	form F $C_4H_5FN_3O^+$, $^1/_2C_4H_2O_4^-$, H_2O
space group $P2_1/c$	space group $P2_1/c$	space group $P2_1/c$
a (Å) = 5.2610(2)	a = 9.3450(5)	a = 3.550(5)
b (Å) = 15.1970(6)	b = 11.8620(6)	b = 9.093(5)
c (Å) = 7.8840(3)	c = 18.9540(8)	c = 24.527(5)
β = (Å) 92.206(3)	β = 113.573(3)	β = 91.737(5)
V (Å^3) = 629.87(4)	V = 1925.73(16)	V = 791.4(12)
Z = 4	Z = 4/Z' = 2	Z = 4
ρ_{calc} = 1.836 g/cm^3	ρ_{calc} = 1.691 g/cm^3	ρ_{calc} = 1.722 g/cm^3
1287 unique reflns	3907 unique reflns	1600 unique reflns
$R_{(int)}$ = 0.0298	$R_{(int)}$ = 0.0570	$R_{(int)}$ = 0.0178
θ_{max} = 26.42°	θ_{max} = 26.37°	θ_{max} = 26.29°
$R_{1[I>2\sigma(I)]}$ = 0.0466	$R_{1[I>2\sigma(I)]}$ = 0.0545	$R_{1[I>2\sigma(I)]}$ = 0.0346
wR_2 = 0.1214	wR_2 = 0.1162	wR_2 = 0.0965
S = 1.046	S = 1.045	S = 1.053

All 5-FC salts crystallize in the monoclinic space group $P2_1/c$ (see Table 1), protonated at the N3 ring position (Figure 1). In Supporting Information Table 2, the main hydrogen-bond geometries for each crystal structure are listed.

3.1.1. Oxalate of 5-FC. The asymmetric unit of form O (Figure 1) exhibits one $(5\text{-FC})^+$ and one $(\text{oxalate})^{-2}$, being the anion placed on a crystallographic 2-fold axis (Figure 1). The main motif $R_2^2(8)$ (Figure 2a) is assembled via complementary N41−H41A···O4 and $N3^+$−H3···$O3^-$ hydrogen bonds between the 5-FC molecule and a half $(\text{oxalate})^-$ ion. Taking into account the presence of an inversion center on the $(\text{oxalate})^{-2}$ ion, we will consider the resulting three-component supermolecule (5-FC−oxalate−5-FC, Figure 2a) as a unit, referring to it as the heterodimer or dimeric unit for the discussion in succession. In this way, the adjacent dimeric units of form O are connected through secondary N1−H1···O4 hydrogen bonds to form a planar layer perpendicular to the *ac* plane. These dimeric units are disposed in a zigzag fashion. A secondary $R_2^2(10)$ motif, constituted by self-complementary N41−H41B···F51 hydrogen bonds (Figure 2a), is observed between the 5-FC molecules belonging to the stacked dimeric units. Finally, the 3D packing of form O is completed by $\pi\cdots\pi$ stacking interactions occurring among adjacent layers, perpendicular to the *ac* plane (Figure 2b), the interlayer distance being of 3.13(2)Å.

3.1.2. Fumarate of 5-FC Monohydrate. The asymmetric unit of form F (Figure 3a) exhibits one $(5\text{-FC})^+$, one $(\text{fumarate})^{-2}$, and one molecule of water, where the anion is placed on a crystallographic 2-fold axis. (Figure 1). As the $(\text{fumarate})^{-2}$ ion also exhibits an inversion center, the heterodimer unit observed in form O is preserved in form F. Thus, the main motif $R_2^2(8)$ (Figure 3a) formed by complementary N41−H41A···O4 and $N3^+$−H···$O3^-$ hydrogen bonds is retained in the crystal packing of form F. Secondary

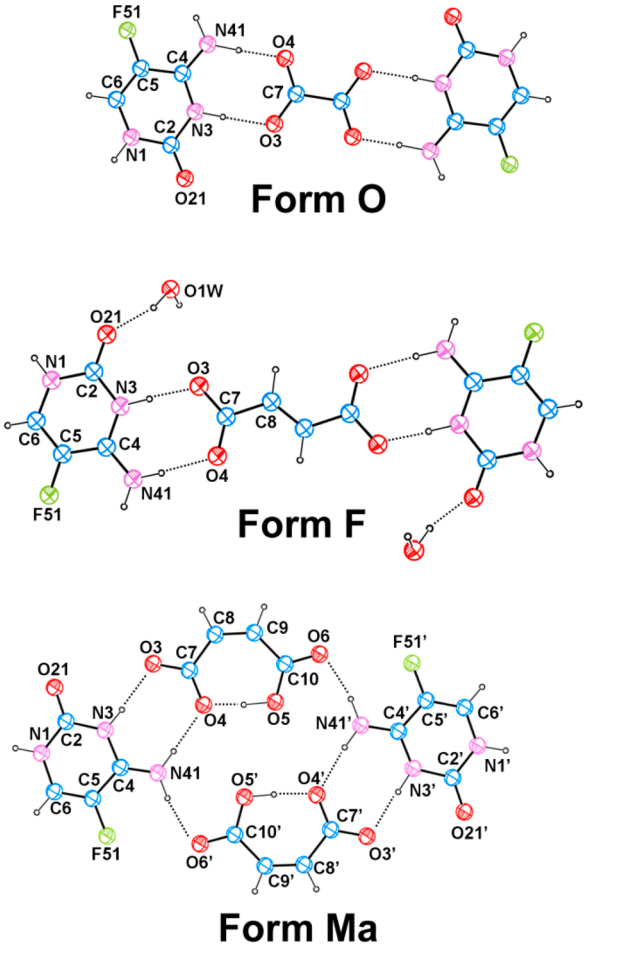

Figure 1. ORTEP-3[20] type view of the asymmetric unit of all 5-FC salts. Thermal ellipsoids are at the 50% probability level. Hydrogen atoms are drawn as spheres of arbitrary radii. Hydrogen bonds are shown as a dashed line.

N41−H41B···O4 hydrogen bonds (Figure 3a) connect adjacent heterodimers to form infinite planar 1D tapes of dimeric units along the *b* axis. The main and secondary H-bond interactions generate a four-component supermolecule ($R_4^2(8)$) as is shown in Figure 3a. The 1D tapes are connected via H-bonds performed by water molecules. Two hydrogen bonds, N1−H1···O1W and O1W−H1W···O21, connect the water molecule with two 5-FC molecules of adjacent 1D tapes (see Figure 3a), forming a layer perpendicular to the *ac* plane (see Figure 3b). One O1W−H2W···O3 hydrogen bond connects the water molecule with a $(\text{fumarate})^{-2}$ ion belonging to the 1D tape of the adjacent layers (Figure 3b). In the layer, it can be observed that the adjacent 1D tapes are disposed in a zigzag fashion and no classical intermolecular interactions occur between them, just one weak C6−H6···O21 hydrogen bonding. In the [100] direction, the adjacent layers generate columns of 1D tapes. Therefore, the water molecules play an important role in the maintenance of the crystalline arrangement of form F. Beyond the presence of water molecules, the 3D packing of form F is completed by $\pi\cdots\pi$ stacking interactions occurring among 1D tapes of the same column, perpendicular to the *ac* plane (Figure 3b), the column interlayer distance being 3.247(4)Å.

3.1.3. Maleate of 5-FC. The asymmetric unit of form Ma exhibits two $(5\text{-FC})^+(\text{maleate})^-$ ionic pairs (Figure 1). The

dx.doi.org/10.1021/cg400662n | Cryst. Growth Des. 2013, 13, 4315−4322

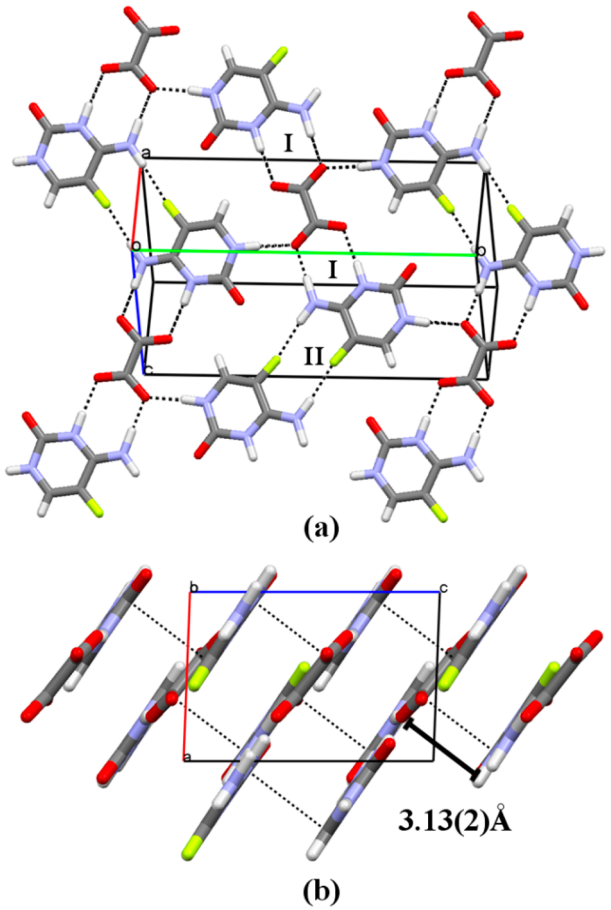

Figure 2. (a) Crystal packing diagram of form O. Dashed lines indicate hydrogen bonds, (I) refers to the $R_2^2(8)$ motif, and (II) refers to the $R_2^2(10)$ motif. (b) Three-dimensional hydrogen-bonded network of form O.

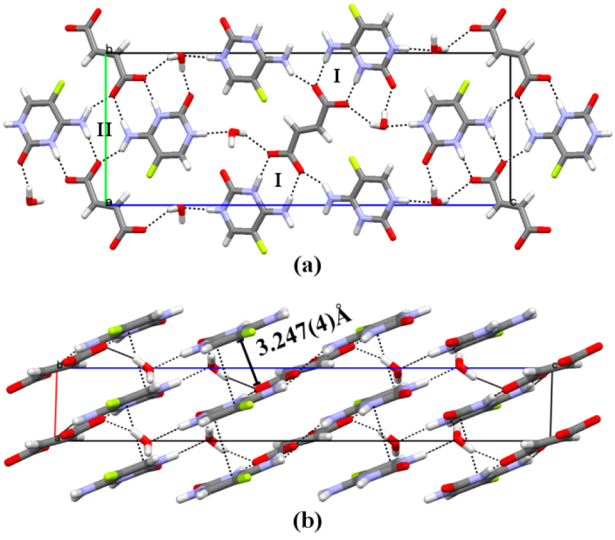

Figure 3. (a) Crystal packing diagram of form F. Dashed lines indicate hydrogen bonds, (I) refers to the $R_2^2(8)$ motif, and (II) refers to the $R_4^2(8)$ motif. (b) Three-dimensional hydrogen-bonded network of form F.

heterodimer of this salt, unlike observed in the forms O and F, is composed by one molecule of 5-FC and one molecule of the $(maleate)^-$ ion, once the ion exhibits no inversion center due to the presence of an intramolecular O−H···O hydrogen bond. Nevertheless, the main motif $R_2^2(8)$ (Figure 4a) is still preserved

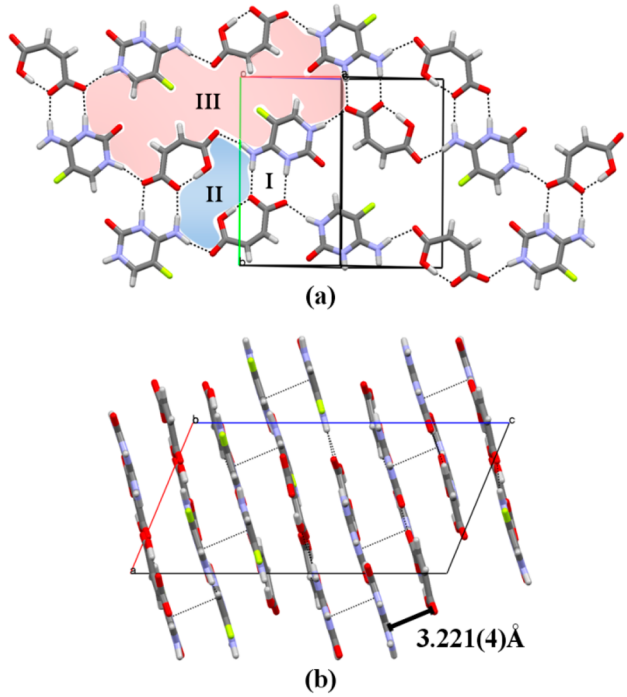

Figure 4. (a) Crystal packing diagram of form Ma. Dashed lines indicate hydrogen bonds, (I) refers to the $R_2^2(8)$ motif, (II) refers to the $R_6^4(16)$ motif, and (III) refers to the $R_8^6(48)$ motif. (b) Three-dimensional hydrogen-bonded network of form Ma.

in one side of the $(maleate)^-$ ion, which exhibits the same complementary N41−H41A···O4 and $N3^+$−H···$O3^-$ hydrogen bond patterns among the 5-FC and the acid (Figure 4a). Two secondary N−H···O hydrogen bonds occur with the $(maleate)^-$ ion and the 5-FC molecules and act in order to form planar layers along the *ab* plane. One of them involves the free hydrogen atom H41B of the amine group of the 5-FC molecule and the oxygen atom O6 of the $(maleate)^-$ ion. Together with the N41−H41A···O4 and the intramolecular O−H···O hydrogen bonds, this secondary hydrogen bond constitutes a ring, composed by the molecules of the asymmetric unit of form Ma, which we will denominate heterotetramer, exhibiting a $R_6^4(16)$ graph-set motif (detached area II in the Figure 4a). The other secondary hydrogen bond involves the N1−H1···O3 atoms and is responsible for connecting adjacent heterotetramers. Every four connected heterotetramers lead to the formation of a bigger ring motif ($R_8^6(48)$) detached area III in the Figure 4a. The absence of water molecules in the crystalline arrangement of form Ma generates a 3D crystal packing similar to the one observed for form O, where $\pi\cdots\pi$ stacking interactions occur between adjacent layers, also perpendicular to the *ac* plane (Figure 4b), with an interlayer distance of 3.221(4)Å.

4. DISCUSSION

5-FC is a rigid molecule, adopting a planar conformation (rms deviation for forms O, F, and Ma molecules A and A′, respectively = 0.0224 Å, 0.0078 Å, 0.0156 Å, and 0.0099 Å for all non-H atoms). When compared to the cytosine pK_a value (pK_a = 4.6),[34] the 5-FC is a weakly basic compound (pK_a = 3.26) due the presence of a most electronegative fluorine atom in its constitution. This substitution attracts the π electrons of

dx.doi.org/10.1021/cg400662n | *Cryst. Growth Des.* 2013, 13, 4315−4322

the N3 nitrogen atom, interfering in its protonation. The fluorination of organic compounds is being increasingly explored in the clinical use, once evidences of improvements in the pharmacokinetic properties of the drugs are being observed. Although halogens are expected to be excellent hydrogen bond acceptors due their high electronegativity, in reality and in particular for the fluorine atom, the propensity to form hydrogen bonds is poor, in a fashion that the organic fluorine acts as an extremely weak base. For this reason, N−H···F intermolecular/intramolecular interactions are rare to occur and only a few examples are found in the literature. Nevertheless, intramolecular N−H···F interactions are observed in all the three salts and an intermolecular N−H···F interaction is observed in the form O. On the basis of the available structural information and on the performed theoretical studies, it is believed that these interactions occur as stabilizing forces inside the crystalline packing and not as a result of close packing. In particular, the intermolecular N−H···F interaction observed in the form O acts as a connector among the heterodimeric units, thus contributing to the stabilization of this salt.[35,36]

By considering that dicarboxylic acids are a class of compounds which exhibit a large range of pK_a values, dicarboxylic acids with opened and closed chains were used in the crystallization experiment in order to evaluate the behavior of the hydrogen bonding patterns in the 5-FC molecule and its potential to form salts or cocrystals. For this purpose, the acids were chosen according to their pK_a values, considering that the ΔpK_a between the acid and the 5-FC were inside the range of the salt−cocrystal continuum, i.e., $0 < \Delta pK_a < 2$. It is worth mentioning that in a first approach, all crystallization experiments were conducted in water solutions to ensure proximity of the intrinsic pK_a value of each compound. Then, variations in the pK_a were promoted by using acetonitrile and 2-propanol, both mixed with water (1:1), to evaluate the behavior and dependence of the 5-FC salt formation in relation to the ΔpK_a. Storage temperature was also considered in this evaluation.

The distinction between salts and cocrystals for carboxylic acids as the crystallizing molecule can be made based on the C−O distance, D_{C-O}.[5] If a $(carboxylate)^-$ is formed, i.e., if a salt is formed, then the C−O distances possesses similar values (1.25 Å[37]) and the ΔD_{C-O} is smaller than 0.03 Å. On the other hand, if there is no ionization, i.e., if a cocrystal is formed, then the neutral carboxyl groups possess different C−O values (1.20 Å[37] and 1.30 Å[37]) and the ΔD_{C-O} is larger than 0.08 Å. By calculating the ΔD_{C-O} for the carboxyl groups of the acid molecules present in the forms O (ΔD_{C-O} = 0.0091(22) Å), F (ΔD_{C-O} = 0.051(16) Å), and Ma (ΔD_{C-O} = 0.0134(28) Å and 0.0102(30) Å), it can be verified that for two of the three salts, the ΔD_{C-O} remains smaller than 0.03 Å, indicating that salts are indeed formed. For form F (ΔpK_a = 0.23), however, the ΔD_{C-O} value indicates that the complex could be a salt or a cocrystal. Although the hydrogen atoms positions are somewhat uncertain when determined from the electron density maps obtained by X-ray diffraction, the proton transfer is observed in the electron density map of form F, being the smaller symmetry in the $(carboxylate)^-$ attributed to the interaction between its oxygen atom and the water molecule trapped into the lattice. This causes a rearrangement of the charge density around the oxygen involved in this interaction that lead to an increase of one of the carboxylic C−O distance to 1.292(2)Å, when it was expected to assume an intermediate bond length of ca. 1.25 Å.[37] The other oxygen−carbon bond of the $(carboxyl)^-$ anion assumes a C−O distance of 1.241(2) Å, which is in agreement with the formation of the anion.

The above results seem to indicate that for the 5-FC case the use of water as the crystallization solvent lead preferentially to the formation of salt in the continuum. However, unpredictable ionization states in the continuum region could occur if, for example, the solvent was changed once the pK_a value changes with different solvents. Nevertheless, even changing the solvents during the crystallization experiments performed with the 5-FC molecules, the salts were still formed, indicating that at least for this molecule, the salt formation in the continuum seems to be a tendency that depends more of the chemical features of the molecule than of the ΔpK_a, which in turn plays an important role in the selection of acid−base pairs and their potential to form salts. In an attempt to state this tendency, quantum mechanical calculations of the energy surface of an isolated acid/5-FC dimeric unit were performed by scanning the $N3^{\delta+}-H\cdots O3^{\delta-}$ interaction to evaluate the energy involved in the proton transition between the carboxylic group and a 5-FC unit. The calculation performed on the forms O and Ma showed that the energy surfaces present their minimum values when the proton is near to the imine nitrogen atom of the 5-FC base-unit when the chemical species are ionized (see Supporting Information). As the proton distance increases, i.e., when the proton gets closer to the carboxylic group, the energies increase linearly reaching its maximum values between 12 and 16 kcal/mol. This values indicate the cocrystal formation is the higher energy state, being the salt forms more stable than the cocrystal forms.

4.1. Supramolecular Analysis. By comparing the supramolecular synthons observed in the 5-FC salts depicted here with the salicylate of 5-FC[14] and with similar synthons found in the Cambridge Structural Database (CSD),[37] a structural preference emerge: the formation of heterosynthons with a $R_2^2(8)$ graph-set motif. According to Allen and Desiraju et al.,[38,39] the $R_2^2(8)$ motif is one of the most recurrently synthons among the crystalline structures. It is expected for complementary compounds, such as carboxylic acids which present donor−acceptor terminal groups and the 5-FC molecule that exhibits two acceptor−donor hydrogen bonding sites, N3:N41 and O21:N1. The heterosynthons are observed in all the salts depicted here and in the 5-FC salt with salycilic acid,[13] involving the same acceptor−donor hydrogen bonding site of the 5-FC molecule, the N3:N41, where the N3 nitrogen atom is protonated in a fashion that the hydrogen atom of the carboxylic group is linked to this atom characterizing the salt formation. In this way, the CSD (version 5.33, with August 2012 updates) motif search,[40] considering the statistics associated with the supramolecular heterosynthon formed with this 5-FC site, was carried out in two steps, within the Materials Mercury tool:[27] one considering the predefined COO···NHCNH2 motif, denominated as raw data in the Figure 5, and another one considering the structures containing exclusively the carboxylic acid group interacting with the 4-aminopyrimidine group, constituting salts, denominated refined data in the Figure 5. Although homosynthons with a $R_2^2(8)$ graph-set motif, composed by carboxylic acid−carboxylic acid or by 4-aminopyrimidine−4-aminopyrimidine groups are also expected to occur, the heterosynthon dominates in the crystalline structures containing similar $R_2^2(8)$ motifs, stated on the basis that 74% of the structures containing both functional groups exhibit the heterosynthon arrangement

dx.doi.org/10.1021/cg400662n | Cryst. Growth Des. 2013, 13, 4315−4322

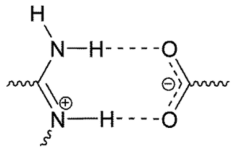

Raw data:

614 entries both COO^- and $HNCNH_2$

454 (74%) entries COO^- ••• $HNCNH_2$ supramolecular heterosynthon

Refined data:

111 entries both COO^- and $(4\text{-aminopyrimidine})^+$

52 (47%) entries COO^- •••$(4\text{-aminopyrimidine})^+$ supramolecular heterosynthon

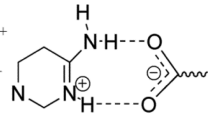

Figure 5. CSD[22,26] statistics associated with the preference of the intermolecular $COO^-/NHCNH_2$ and the $COO^-/(4\text{-aminopyrimidine})^+$ interactions to form heterosynthons.

(Figure 5). For the two chloride monohydrate of 5-FC,[7,13] such a heterosynthon is not observed once it is one halide (Cl) which protonates the N3 atom of the 5-FC molecule. However, in one of the chloride monohydrate structures,[13] the hydrogen bonding pattern shows intermolecular interactions between the 5-FC molecules similar to the CG Watson and Crick base pairing, evidencing a third acceptor−acceptor−donor hydrogen bonding site available in the 5-FC molecule for salt formation, the O21−N3−N41.

4.2. Thermal Analysis. The DSC thermal curve of the raw 5-FC shows a sharp endothermic peak at T_{onset} = 297.81 °C, which is in agreement with its reported melting point[15] (see Figure 6a). This event is followed by an intense exothermal effect, attributed to the drug decomposition process. This same thermal behavior is observed in the DSC curves of the forms F, O, and Ma (Figure 6b,c,d, respectively). The forms O and Ma exhibit only one peak, at 253.73 and 198.29 °C, respectively, associated to the fusion/decomposition of the compound. The form F, on the other hand, exhibits two peaks, one at 98.29 °C, associated to a not reversible process of water loss (confirmed by TGA, see Supporting Information) and another one at 236.44 °C, associated the fusion/decomposition of the compound. Commonly, salt formation is applied to improve stability of APIs by increasing its melting point, but according to the DSC experiments (Figure 6), the salt formation of the 5-FC molecule is decreasing its melting point. For forms F and Ma, the melting point decreases more than 55 °C. In the form O, however, where the acid molecule exhibits the smaller pK_a value, thus forming the strongest salt, the melting point is about 25 °C below the one observed for the free base and the behavior during the decomposition process is closer to sublimation instead of boiling as observed in the forms F and Ma decomposition.

4.3. X-ray Diffraction Analysis. X-ray powder diffractograms of the forms F, Ma, and O were made for two reasons in this work: to verify the sample purity after the crystallization process and to verify the stability of the form F after the water loss. All the calculated and experimental X-ray powder diffractograms are in good agreement (see Supporting Information Figure 7), stating the purity of the compounds, which is one of the most important features that must be achieved during the synthesis of a new solid form of an API. Concerning the form F, once the molecules of water are strongly linked into the crystalline lattice, trapped by O−H···O and N−H···O hydrogen bonds, the diffractogram shows that this compound suffers a partial amorphization process after the water loss. However, even with an amorphous phase emerging, it still preserves some peaks, indicating that a small amount of crystallinity is preserved (see Supporting Information Figure 7).

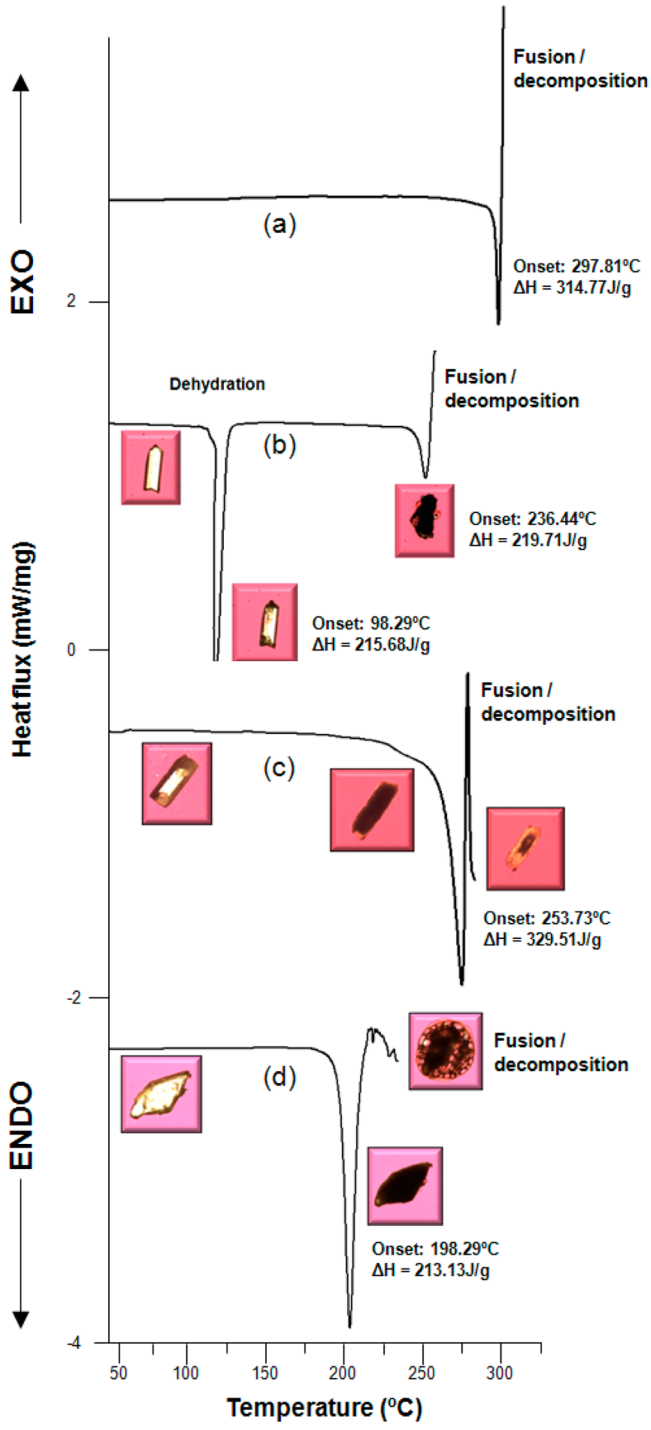

Figure 6. DSC curves and crystal behavior visually checked by hot-stage microscopy of the (a) free base, (b) form F, (c) form O, and (d) form Ma.

Nevertheless, the peaks recorded after the water loss suggest the formation of a new phase, probably a dehydrated one, once the peaks do not overlap neither with the fumaric acid nor with the 5-FC powder diffractograms by themselves. Until the present, we were unable to synthesize the dehydrated form of the form F, which would allow us to confirm our hypothesis.

4.4. Vibrational Analysis. To support the intermolecular interactions determined by single crystal X-ray diffraction, FT-IR and Raman scattering experiments were conducted (see Supporting Information Figure 8). A detailed discussion of the

dx.doi.org/10.1021/cg400662n | Cryst. Growth Des. 2013, 13, 4315−4322

vibrational spectra of 5-FC was reported by Seshadri et al.[41] and Jaworski et al.[42] The main spectral features of the 5-FC molecule can be easily identified in the three salts. For example, the breathing mode of the aromatic ring is clearly identified at 780 cm^{-1} and the in-plane deformation of the C−H and N−H are observed between 1200 and 1400 cm^{-1}. However, differences in the molecular environment and intermolecular interactions lead to univocal features which can be associated to the new crystal forms. The carbonyl group usually fingerprints the intermolecular interactions due to its participation in hydrogen bonds. That is the case of the crystalline structure of 5-FC[28] and, as a consequence, the ν(C2O21) stretching is shifted toward lower wavenumbers (1675 cm^{-1}). On the other hand, this moiety does not play a relevant role in the crystal packing of the 5-FC salts, which exhibit the ν(C2O21) at a higher wavenumber (~1715 cm^{-1}). However, the 5-FC carbonyl bands are overlapped with those of the carboxylic acid and it is not possible to perform an accurate assignment. Another interesting signature of the 5-FC spectra is the ν(C6H) stretching (3091 cm^{-1}), which is observed at different wavenumbers in forms O (3095 cm^{-1}) and F (3087 cm^{-1}), whereas it is split in form Ma (3061/3070 cm^{-1}) due to the two 5-FC molecules in the asymmetric unit. The C6H group is not involved in the main hydrogen bond pattern but exhibit single (5-FC and form Ma) and bifurcated (form O and form F) short contacts (see Supporting Information Table 2). In particular, the lower wavenumbers observed in form Ma is well correlated with the shortest C6H···X intermolecular distance among the 5-FC salts reported in this contribution. Finally, the ν(NH) stretching modes need to be considered because the corresponding bonds are essential in stabilizing the crystalline structure. These modes are spread between 3100 and 3450 cm^{-1}, mainly due to the red-shift induced by the hydrogen bonds. In the case of form O, a very sharp band is observed at 3450 cm^{-1}, which could be associated to the ν(N41−H41B) because it is weakly bonded to fluorine atoms (see Supporting Information Table 2). In the remaining structures, including the one of 5-FC,[15] N41H41B is linked to strongest acceptors, increasing the red-shift and inducing wider bands. Our results show that vibrational spectroscopy was successful to provide distinctive spectral signatures, confirming the intermolecular interactions characteristic of the 5-FC salts.

5. CONCLUSION

According to the salt−cocrystal study, salts are formed when the ΔpK_a among the API and the molecules crystallized with it are higher than 2. When the $0 < \Delta pK_a < 2$, the charge transfer analysis is difficult to predict and it is often performed on the basis of the C−O bond lengths differences, for carboxylic acids in particular. In this study, salts of the API 5-FC were obtained with fumaric, maleic, and oxalic carboxylic acids, first in water solutions, with the system exhibiting ΔpK_a values of 0.23, 1.35, and 2.01, respectively. The experiments were repeated varying the storage temperature and the solutions, leading all of them to the same salts formation results. These results, together with theoretical calculations performed over the free molecule and over the new salts, points to a tendency of this drug do form salts in the continuum. For this particular case, this tendency depends more on the chemical features of the 5-FC molecules than on the ΔpK_a. In this way, together with the consideration about the ΔpK_a, it is believed that tendencies for a given molecule in the continuum might be assigned when complementary experimental and/or theoretical physicochemical studies are considered and explored.

All the salts reported here show a similar hydrogen-bond pattern interactions, complementary to those of 5-FC, protonating its N3 nitrogen atom and forming a $R_2^2(8)$ motifs formed essentially by the same N−H···O hydrogen bond among the acid and the API. According to the DSC experiments, the salt formation reduced the melting point of the solid. This effect suggests that the presence of protonated 5-FC into a crystalline arrangement could improve the physicochemical properties of compounds with dissolution rate/solubility problems.

■ ASSOCIATED CONTENT

Ⓢ Supporting Information

Crystallographic data of 5-FC salts, differential scanning calorimetry and thermogravimetric curves, powder X-ray diffraction pattern, quantum mechanical calculations. This material is available free of charge via the Internet at: http://pubs.acs.org/.

■ AUTHOR INFORMATION

Corresponding Author

*Phone: +55 16 3373 8096. Fax: +55 16 3373 9881. E-mail: javiere@ifsc.usp.br.

Notes

The authors declare no competing financial interest.

■ ACKNOWLEDGMENTS

The authors thank CAPES (C.C.P.S. and J.C.T.), CNPq (J.E., R.O and A.P.A.) and FAPESP for the financial support.

■ REFERENCES

(1) Bond, A. D. In *Pharmaceutical Salts and Cocrystals*; Wouters, J., Quéré, L., Eds.; Royal Society of Chemistry: Cambridge, UK, 2012, Chapter 2, pp 9−28.
(2) Aateka, P.; Stuart, A. J.; Albert, F.; Nilesh, P. *Br. J. Cardiol.* **2009**, *16* (6), 281−286.
(3) Clarke, H. D.; Hickey, M. B.; Moulton, B.; Perman, J. A.; Peterson, M. L.; Wojtas, Ł.; Almarsson, Ö.; Zaworotko, M. J. *Cryst. Growth Des.* **2012**, *12* (8), 4194−4201.
(4) Childs, S. L.; Stahly, G. P.; Park, A. *Mol. Pharmaceutics* **2007**, *4* (3), 323−338.
(5) Bhogala, B. R.; Basavoju, S.; Nangia, A. *CrystEngComm* **2005**, *7*, 551−562.
(6) Ebenezer, S.; Muthiah, P. T. *Cryst. Growth Des.* **2012**, *12* (7), 3766−3785.
(7) Perumalla, S. R.; Pedireddi, V. R.; Sun, C. C. *Cryst. Growth Des.* **2013**, *13* (2), 429−432.
(8) Vermes, A.; Guchelaar, H.-J.; Dankert, J. *J. Antimicrob. Chemother.* **2000**, *46* (2), 171−179.
(9) Kim, K.-H.; Kim, J.-Y.; Lee, K.-H.; Noh, M.-J.; Kim, Y.-C.; Park, H.-J. *Bioorg. Med. Chem. Lett.* **2002**, *12* (3), 483−486.
(10) Longley, D. B.; Paul Harkin, D.; Johnston, P. G. *Nature* **2003**, *3*, 330−338.
(11) Nishiyama, T.; Kawamura, Y.; Kawamoto, K.; Matsumura, H.; Yamamoto, N.; Ito, T.; Ohyama, A.; Katsuragi, T.; Sakai, T. *Cancer Res.* **1985**, *45* (4), 1753−1761.
(12) Xu, G.; McLeod, H. L. *Clin. Cancer Res.* **2001**, *7* (11), 3314−24.
(13) Prabakaran, P.; Murugesan, S.; Muthiah, P. T.; Bocelli, G.; Righi, L. *Acta Crystallogr., Sect. E: Struct. Rep. Online* **2001**, *57* (10), o933−o936.
(14) Portalone, G.; Colapietro, M. *J. Chem. Cryst.* **2007**, *37* (2), 141−145.

(15) Hulme, A. T.; Tocher, D. A. *Cryst.Growth Des.* **2006**, *6* (2), 481−487.
(16) Portalone, G.; Colapietro, M. *Acta Crystallogr., Sect. E: Struct. Rep. Online* **2006**, *62* (3), o1049−o1051.
(17) Tutughamiarso, M.; Bolte, M.; Egert, E. *Acta Crystallogr., Sect. C: Cryst. Struct. Commun.* **2009**, *65* (11), o574−o578.
(18) Hulme, A. T.; Tocher, D. A. *Acta Crystallogr., Sect. E: Struct. Rep. Online* **2005**, *61* (7), 02112−o2113.
(19) Louis, T.; Low, J. N.; Tollin, P. *Cryst. Struct. Commun.* **1982**, *11*, 1059−1064.
(20) Portalone, G. *Chem. Cent. J.* **2011**, *5* (51), 1−8.
(21) Tutughamiarso, M.; Wagner, G.; Egert, E. *Acta Crystallogr., Sect. B: Struct. Sci.* **2012**, *B68* (4), 431−443.
(22) Tutughamiarso, M.; Egert, E. *Acta Crystallogr., Sect. B: Struct. Sci.* **2012**, *B68* (4), 444−452.
(23) *COLLECT*; Data Collection Software; Nonius: Delft, The Netherlands, 1998.
(24) Otwinowski, Z.; Minor, W. In *Methods in Enzymology: Macromolecular Crystallography*; Carter, C. W., Jr., Sweet, R. M., Eds.; Academic Press: New York, 1997, Part A, Vol. *276*, pp 307−326.
(25) Sheldrick, G. M. *Acta Crystallogr., Sect. A: Found. Crystallogr.* **2008**, *A64*, 112−122.
(26) Farrugia, L. J. *J. Appl. Crystallogr.* **2012**, *45*, 849−854.
(27) Macrae, C. F.; Bruno, I. J.; Chisholh, J. A.; Edgington, P. R.; McCabe, P.; Pidcock, E.; Rodriguez-Monge, L.; Taylor, R.; van de Streek, J.; Wood, P. A. *J. Appl. Crystallogr.* **2008**, *41*, 466−470.
(28) Farrugia, L. J. *J. Appl. Crystallogr.* **1997**, *30*, 565.
(29) Parr, R. G.; Yang, W. *Density Functional Theory of Atoms and Molecules*; Oxford University Press: New York, 1989.
(30) Lee, C. T.; Yang, W. T.; Parr, R. G. *Phys. Rev. B* **1988**, *37*, 785−789.
(31) Becke, A. D. *J. Chem. Phys.* **1993**, *98*, 5648−5652.
(32) Møller, C.; Plesset, M. S. *Phys. Rev.* **1934**, *46*, 618−622.
(33) Frisch, M. J.; Trucks, G. W.; Schlegel, H. B.; Scuseria, G. E.; Robb, M. A.; Cheeseman, J. R.; Montgomery, J. A., Jr.; Vreven, T.; Kudin, K. N.; Burant, J. C.; Millam, J. M.; Iyengar, S. S.; Tomasi, J.; Barone, V.; Mennucci, B.; Cossi, M.; Scalmani, G.; Rega, N.; Petersson, G. A.; Nakatsuji, H.; Hada, M.; Ehara, M.; Toyota, K.; Fukuda, R.; Hasegawa, J.; Ishida, M.; Nakajima, T.; Honda, Y.; Kitao, O.; Nakai, H.; Klene, M.; Li, X.; Knox, J. E.; Hratchian, H. P.; Cross, J. B.; Adamo, C.; Jaramillo, J.; Gomperts, R.; Stratmann, R. E.; Yazyev, O.; Austin, A. J.; Cammi, R.; Pomelli, C.; Ochterski, J. W.; Ayala, P. Y.; Morokuma, K.; Voth, G. A.; Salvador, P.; Dannenberg, J. J.; Zakrzewski, V. G.; Dapprich, S.; Daniels, A. D.; Strain, M. C.; Farkas, O.; Malick, D. K.; Rabuck, A. D.; Raghavachari, K.; Foresman, J. B.; Ortiz, J. V.; Cui, Q.; Baboul, A. G.; Clifford, S.; Cioslowski, J.; Stefanov, B. B.; Liu, G.; Liashenko, A.; Piskorz, P.; Komaromi, I.; Martin, R. L.; Fox, D. J.; Keith, T.; M. A. Al-Laham, Peng, C. Y.; Nanayakkara, A.; Challacombe, M.; Gill, P. M. W.; Johnson, B.; Chen, W.; Wong, M. W.; Gonzalez, C.; Pople, J. A. *Gaussian 03*, revision C.02;Gaussian Inc.: Wallingford, CT, 2004.
(34) Bossche, H. V.; Willemsens, G.; Marichal, P. *Crit. Rev. Microbiol.* **1987**, *15*, 57−72.
(35) Sunil, S. L.; Nayak, S. K.; hathwar, V. R.; Chopra, D.; Row, T. N. In *Pharmaceutical Salts and Cocrystals*, Wouters, J., Quéré, L., Eds.; Royal Society of Chemistry: Cambridge, UK, 2012, Chapter 3, pp 29−43.
(36) Desiraju, G.; Steiner, T. The Weak Hydrogen Bond. *Structural Chemistry and Biology*; Desiraju, G., Steiner, T., Eds.; Oxford University Press Inc.: New York, 1999, Chapter 3, pp 202−215.
(37) Allen, F. H. *Acta Crystallogr., Sect. B: Struct. Crystallogr. Cryst. Chem.* **2002**, *58*, 380−388.
(38) (a) Allen, F. H.; Raithby, P. R.; Shields, G. P.; Taylor, R. *Chem. Commun.* **1998**, *9*, 1043−1044. (b) Allen, F. H.; Motherwell, W. D. S.; Raithby, P. R.; Shields, G. P.; Taylor, R. *New J. Chem.* **1999**, *23*, 25−34.
(39) Desiraju, G. R. *Angew. Chem., Int. Ed. Engl.* **2003**, *34*, 2311−2327.
(40) Shan, N.; Zaworotko, M. *Drug Discovery Today* **2008**, *13* (9/10), 440−446.
(41) Seshadri, S.; Gunasekaran, S.; Muthu, S.; Kumaresan, S.; Arunbalaji, R. *J. Raman Spectrosc.* **2007**, *38* (11), 1523−1531.
(42) Jaworski, A.; Szczesniak, M.; Szczepaniak, K.; Kubulat, K.; Person, W. B. *J. Mol. Struct.* **1990**, *223*, 63−92.